A Genetic Variant BDNF Polymorphism Alters Extinction Learning in Both Mouse and Human

Fatima Soliman, *et al.*

Science **327**, 863 (2010);
DOI: 10.1126/science.1181886

identical MIS 5e/5a relative sea-level histories of tectonically stable Bermuda and Mallorca. The very rapid onset and relatively brief nature of the MIS 5a highstand may have plausibly generated lags between the timing of sea-level changes and the timing of coral reef growth, and may provide a partial explanation as to why reefs on Barbados and New Guinea do not record a comparable eustatic height for this event. This and other factors that could be part of the apparent discrepancy are discussed in (*9*).

The suggestion that MIS 5a sea level was slightly higher than at present and only slightly lower than the MIS 5e sea level implies that most of the ice built up during MIS 5b would have melted during the onset of MIS 5a. The ~84- to 80-ka timing of this highstand closely matches the June 60°N insolation peak at ~84 ka (Fig. 2E), a pattern that is consistent with the Milankovitch model. In fact, June insolation at 60°N was higher at ~84 ka than that at 11 ka (*27*), and field studies in the Baffin Island region suggest the complete melting of the Laurentide Ice Sheet around 80 ka (*28*). Finally, we find additional, independent support for a near-modern eustatic MIS 5a highstand when we consider the indirect sea-level estimate of (*29*) inferred from a Pacific benthic $\delta^{18}O$ record, the Vostok atmospheric $\delta^{18}O$ record, and certain assumptions about the Dole effect on deep-water temperatures (Fig. 2D). The premise of the approach of (*29*) is that the deep-sea $\delta^{18}O$ record does not capture the true magnitude of eustatic sea-level change, because the $\delta^{18}O$ signal is partially controlled by temperature.

Because of its relation to continental ice volume, an accurate Quaternary sea-level curve has been a long-term goal of scientists interested in ice-age cycles and their causes. Ice-age theory has long assumed gradual ice buildup and more rapid ice melting in the generally accepted model of the ~100-ky cycle of glaciation. Instead, the emerging body of evidence suggests that both melting and accumulation can be very rapid during discrete intervals of time when specific conditions prevail. Furthermore, the 100-ky model of glaciation has always faced the problem that although the deep-sea $\delta^{18}O$ record is dominated by a 100-ky cycle, northern high-latitude summer insolation has negligible power in this band. Our data from Mallorca and data from other sites around the world indicate the possibility that eustatic sea level was near modern levels at ~80 ka. If this is true, the 100-ky cycle so universally accepted as the main rhythm of the Middle and Late Quaternary glaciations, in fact, applies rather poorly to ice growth and decay, but much better to carbon dioxide, methane, and temperatures recorded by polar ice (*30*).

References and Notes

1. P. J. Hearty, *Quat. Sci. Rev.* **6**, 245 (1987).
2. C. D. Gallup, R. L. Edwards, R. G. Johnson, *Science* **263**, 796 (1994).
3. K. Lambeck, J. Chappell, *Science* **292**, 679 (2001).
4. D. R. Muhs, K. R. Simmons, B. Steinke, *Quat. Sci. Rev.* **21**, 1355 (2002).
5. E. K. Potter, K. Lambeck, *Earth Planet. Sci. Lett.* **217**, 171 (2003).
6. J. F. Wehmiller *et al.*, *Quaternary Int.* **120**, 3 (2004).
7. J. Ginés, *Endins* **20**, 71 (1995).
8. P. Tuccimei *et al.*, *Earth Surf. Process. Landf.* **35**, (2010).
9. Materials, methods, and additional discussion are available as supporting material on *Science* Online.
10. P. Tuccimei *et al.*, *Z. Geomorphol.* **50**, 1 (2006).
11. R. E. Dodge, R. G. Fairbanks, L. K. Benninger, F. Maurrasse, *Science* **219**, 1423 (1983).
12. T. M. Esat, M. T. McCulloch, J. Chappell, B. Pillans, A. Omura, *Science* **283**, 197 (1999).
13. W. X. Li *et al.*, *Nature* **339**, 534 (1989).
14. M. A. Toscano, J. Lundberg, *Quat. Sci. Rev.* **18**, 753 (1999).
15. J. X. Mitrovica, G. A. Milne, *Quat. Sci. Rev.* **21**, 2179 (2002).
16. P. A. Pirazzoli, *Quat. Sci. Rev.* **24**, 1989 (2005).
17. K. Lambeck, M. Azidei, F. Antonioli, A. Benini, A. Esposito, *Earth Planet. Sci. Lett.* **224**, 563 (2004).
18. W. R. Peltier, *Annu. Rev. Earth Planet. Sci.* **32**, 111 (2004).
19. P. Stocchi, G. Spada, *Ann. Geophys.* **50**, 741 (2007).
20. E. J. Hodge, D. A. Richards, P. L. Smart, A. Ginés, D. P. Mattey, *J. Quat. Sci.* **23**, 713 (2008).
21. R. L. Edwards *et al.*, *Science* **260**, 962 (1993).
22. P. J. Hearty, *Quat. Sci. Rev.* **17**, 333 (1998).
23. K. R. Ludwig, D. R. Muhs, K. R. Simmons, R. B. Halley, E. A. Shinn, *Geology* **24**, 211 (1996).
24. H. L. Vacher, P. Hearty, *Quat. Sci. Rev.* **8**, 159 (1989).
25. M. K. Coyne, B. Jones, D. Ford, *Quat. Sci. Rev.* **26**, 536 (2007).
26. D. R. Muhs, J. F. Wehmiller, K. R. Simmons, L. L. York, in *The Quaternary Period in the United States*, A. R. Gillespie, S. C. Porter, B. F. Atwater, Eds. (Elsevier, Amsterdam, 2004), pp. 147–183.
27. A. Berger, M. F. Loutre, *Quat. Sci. Rev.* **10**, 297 (1991).
28. G. H. Miller *et al.*, *Quat. Sci. Rev.* **18**, 789 (1999).
29. N. J. Shackleton, *Science* **289**, 1897 (2000).
30. J. R. Toggweiler, *Paleoceanography* **23**, PA2211 (2008).

31. This material is based on work supported by NSF (grant OISE-0826667 to B.P.O. and J.A.D.), the University of South Florida (grant R058889) to B.P.O., and the MICINN-FEDER Projects CGL2006-11242-C03-01 and CGL2009-07392 of the Spanish Government to J.J.F. We thank L. Vacher, V. Polyak, and E. A. Bettis III for stimulating discussions, three anonymous reviewers for insightful criticism that considerably improved the manuscript, and F. Gràcia and K. Downey for some of the pictures.

Supporting Online Material

www.sciencemag.org/cgi/content/full/327/5967/860/DC1
Materials and Methods
SOM Text
References

9 September 2009; accepted 7 January 2010
10.1126/science.1181725

A Genetic Variant BDNF Polymorphism Alters Extinction Learning in Both Mouse and Human

Fatima Soliman,[1,2]* Charles E. Glatt,[2] Kevin G. Bath,[2] Liat Levita,[1,2] Rebecca M. Jones,[1,2] Siobhan S. Pattwell,[2] Deqiang Jing,[2] Nim Tottenham,[1,2] Dima Amso,[1,2] Leah H. Somerville,[1,2] Henning U. Voss,[3] Gary Glover,[4] Douglas J. Ballon,[3] Conor Liston,[1,2] Theresa Teslovich,[1,2] Tracey Van Kempen,[1,2] Francis S. Lee,[2]* B. J. Casey[1,2]*

Mouse models are useful for studying genes involved in behavior, but whether they are relevant to human behavior is unclear. Here, we identified parallel phenotypes in mice and humans resulting from a common single-nucleotide polymorphism in the brain-derived neurotrophic factor (BDNF) gene, which is involved in anxiety-related behavior. An inbred genetic knock-in mouse strain expressing the variant BDNF recapitulated the phenotypic effects of the human polymorphism. Both were impaired in extinguishing a conditioned fear response, which was paralleled by atypical frontoamygdala activity in humans. Thus, this variant BDNF allele may play a role in anxiety disorders showing impaired learning of cues that signal safety versus threat and in the efficacy of treatments that rely on extinction mechanisms, such as exposure therapy.

Genetically modified mice provide useful model systems for testing the role of candidate genes in behavior. The extent to which such genetic manipulations in the mouse and the resulting phenotype can be translated across species, from mouse to human, is less clear. In this report, we focused on identifying biologically valid phenotypes across species. We utilized a common single-nucleotide polymorphism (SNP) in the brain-derived neurotrophic factor (BDNF) gene that leads to a valine (Val) to methionine (Met) substitution at codon 66 (Val66Met). In an inbred genetic knock-in mouse strain that expresses the variant BDNF allele to recapitulate the specific phenotypic properties of the human polymorphism in vivo, we found the BDNF Val66Met genotype was associated with treatment-resistant forms of anxiety-like behavior (*1*). The objective of this study was to test if the Val66Met genotype could affect extinction learning in our mouse model and whether such findings could be generalized to human populations.

[1]The Sackler Institute for Developmental Psychobiology, Weill Cornell Medical College, New York, NY 10065, USA. [2]Department of Psychiatry, Weill Cornell Medical College, New York, NY 10065, USA. [3]Citigroup Biomedical Imaging Center, Department of Radiology, Weill Cornell Medical College, New York, NY 10065, USA. [4]Lucas Center for Imaging, Department of Radiology, Stanford University, Stanford, CA 94305, USA.

*To whom correspondence should be addressed. E-mail: fas2002@med.cornell.edu (F.S.) or fslee@med.cornell.edu (F.S.L.) or bjc2002@med.cornell.edu (B.J.C.)

BDNF mediates synaptic plasticity associated with learning and memory (*2*, *3*), specifically in fear learning and extinction (*4*, *5*). BDNF-dependent forms of fear learning have known biological substrates and lie at the core of a number of clinical disorders (*6*, *7*) associated with the variant BDNF (*8*–*10*). Fear-learning paradigms require the ability to recognize and remember cues that signal safety or threat and to extinguish these associations when they no longer exist. These abilities are impaired in anxiety disorders such as posttraumatic stress disorder and phobias (*11*, *12*). Behavioral treatments for these disorders such as exposure therapy rely on basic principles of extinction learning (*13*) in which an individual is repeatedly exposed to an event that was previously associated with aversive consequences. Understanding the effect of the BDNF Met allele on these forms of learning can provide insight into the mechanism of risk for anxiety disorders, can refine existing treatments, and may lead to genotype-based personalized medicine.

We examined the impact of the variant BDNF on classic fear conditioning and extinction paradigms that were adapted to be suitable for each species and that are associated with well-known underlying biological substrates (*14*, *15*, *16*). Fear conditioning consisted of pairing a neutral cue with an aversive stimulus. With repeated pairings, the cue itself takes on properties of the aversive stimulus as it predicts threat of an impending aversive event. Extinction consisted of presenting the cue alone following conditioning, whereby the association is diminished with repeated exposure to empty threat.

We tested 68 mice (17 $BDNF^{Val/Val}$, 33 $BDNF^{Val/Met}$ and 18 $BDNF^{Met/Met}$) and 72 humans group-matched for age, gender, and ethnic background (36 Met allele carriers: 31 Val/Met and 5 Met/Met, and 36 non–Met allele carriers: Val/Val) (table S1). We found no effect of the BDNF Met allele on fear conditioning in mice as measured by the percentage of time spent freezing in response to the conditioned stimulus ($F_{2,65} = 1.58$, $P < 0.22$) (fig. S1A) or on general fear arousal as measured by freezing during the intertrial interval (fig. S2). We grouped human Met allele carriers together (Val/Met and Met/Met) for analyses, because the rarity of human Met allele homozygotes prevents enough observations for meaningful analysis. As we found in the mouse, there was no effect of the BDNF Met allele on fear conditioning in humans as measured by skin conductance response to the cue predicting the aversive stimulus relative to a neutral cue ($F_{1,70} = 0.67$, $P < 0.42$) (fig. S1B).

Analysis of extinction trials showed a main effect of genotype for both mice [($F_{2,65} = 6.55$, $P < 0.003$); Val/Val, 48.8 ± 2.3; Val/Met, 53.2 ± 1.8; Met/Met, 61.3 ± 2.8] and humans [($F_{1,70} = 4.86$, $P < 0.03$); Val/Val, 0.32 ± 0.03; Val/Met, 0.42 ± 0.04], such that extinction learning was impaired in Met allele carriers relative to non–Met allele carriers. The Met allele carriers showed slower extinguishing, as indicated by an interaction of time × genotype for the mouse ($F_{2,65} = 6.51$, $P < 0.003$) with no differences in freezing initially, but a dose response of the Met allele on the percentage of freezing behavior during late trials [Val/Val versus Val/Met: $t(48) = –2.62$, $P < 0.01$; Val/Val versus Met/Met: $t(33) = –4.78$, $P < 0.0001$; Val/Met versus Met/Met: $t(49) = –2.90$, $P < 0.006$] (Fig. 1A). Humans showed a similar pattern to the mice with no genotypic difference in the initial human skin conductance response during early trials of extinction [$t(70) = –1.57$, $P < 0.12$], but significant differences by late trials [$t(70) = –2.43$, $P < 0.02$, corrected for time] (Fig. 1B). These data demonstrate slower or impaired extinction related to the Met allele in both mouse and human.

The learning paradigm for humans included a conditioned stimulus paired with the aversive stimulus and a neutral stimulus that was not paired with the aversive stimulus. This design allowed for distinguishing between effects due to impaired learning versus a general effect of heightened anxiety, as generalized heightened anxiety would lead to a similar response to both the conditioned and neutral cues. Met allele carriers had an overall heightened response to both conditioned and neutral cues [main effect of genotype ($F_{1,70} = 7.21$, $P < 0.009$)], but overall, they differentiated between the conditioned and neutral cues similarly to the non–Met allele carriers (fig. S1B). Yet, when we examined these effects over time, Met allele carriers took longer to recognize that the neutral cue was not associated with the aversive stimulus, as evidenced by significant genotypic differences during late trials [$t(70) = –3.46$, $P < 0.001$, corrected for time] but not early trials [$t(70) = –1.44$, $P < 0.16$] (Fig. 2). Thus, the skin conductance response to the neutral cue during fear conditioning showed a pattern similar to that observed during extinction trials (*16*).

The genetic findings for both fear conditioning and extinction suggest that learning about cues that signal threat of an impending aversive event is intact in Met allele carriers. However, learning that cues no longer signal threat (e.g., extinction) or do not predict threat (cues not paired with an aversive stimulus) is impaired in Met allele carriers, which leads to exaggerated and longer retention of aversive responses where they are not warranted.

To provide neuroanatomical evidence to validate our cross-species translation, we used human functional magnetic resonance imaging (MRI) to define the underlying neural circuitry of the behavioral effects of BDNF Val66Met and to map them to known circuits involved in fear learning in the rodent (table S2). We targeted frontoamygdala circuitry that has been demon-

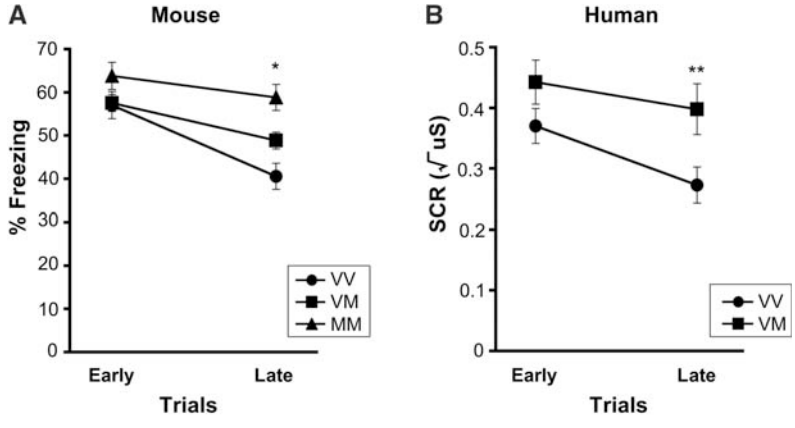

Fig. 1. Altered extinction in mice and humans with BDNF Val66Met. Impaired extinction in Met allele carriers (Val/Met and Met/Met) as a function of time in 68 mice (**A**) and 72 humans (**B**) as indexed by percentage of time freezing in mice and skin conductance response (SCR) in humans to the conditioned stimulus when it was no longer paired with the aversive stimulus. All results are presented as means ± SEM. *$P < 0.01$, Student's *t* test. **$P < 0.02$, Student's *t* test. VV, Val/Val; VM, Val/Met; and MM, Met/Met.

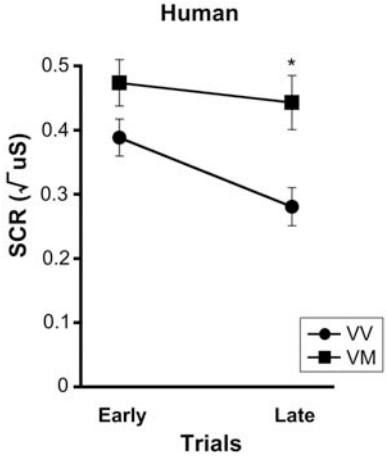

Fig. 2. Impaired learning of neutral cue in human Met allele carriers. Elevated skin conductance response (SCR) to the cue never paired with the aversive stimulus during fear conditioning as a function of time in Met allele carriers (VM) relative to non–Met allele carriers (VV). All results are presented as means ± SEM. *$P < 0.001$, Student's *t* test. VV, Val/Val; VM, Val/Met.

strated to support fear conditioning and extinction in both rodent (*17*–*20*) and human (*21*–*26*) studies. Whereas portions of the amygdala have been shown to be essential for fear conditioning (*27*, *28*), ventral prefrontal cortical regions have been shown to be important for modifying previously learned associations and extinction (*19*, *29*). Thus, on the basis of our behavioral findings in the mouse and human, we hypothesized that ventromedial prefrontal regions, important in extinction, would be less active in Met allele carriers relative to non–Met allele carriers and that amygdala activity may be enhanced.

To test this hypothesis, we examined the main effect of genotype on brain activity during extinction of the previously conditioned stimulus. The analysis directly parallels the observed behavioral main effects of genotype on extinction as measured by mean percentage of time freezing in the mice (Fig. 3A) and mean skin conductance response in humans (Fig. 3B) (*16*) with Met allele carriers showing weaker extinction. The imaging results showed significantly less ventromedial prefrontal cortical (vmPFC) activity during extinction in Met allele carriers relative to non–Met allele carriers [$t(68) = -3.78$, $P < 0.05$, corrected] (Fig. 3C) (*16*). In contrast, Met allele carriers show greater amygdala activity relative to non–Met allele carriers during extinction [$t(68) = 2.23$, $P < 0.05$, corrected] (Fig. 3D). These findings indicate that cortical regions previously shown to be essential for extinction (vmPFC) in both rodent and human (*19*, *26*, *30*) are hyporesponsive in Met allele carriers relative to non–Met allele carriers. Moreover, Met allele carriers show continued recruitment of the amygdala, a region that should show diminished activity during the extinction trials of the experiment (*26*). These findings are most likely due to the SNP biasing activity-dependent learning rather than affecting CNS development per se, as there was no evidence of genotypic developmental effects on brain structure in this ethnicity-, age-, and gender-matched sample from MRI-based brain morphometry (supporting online text). Furthermore, an association between vmPFC activity and the strength of fibers connecting frontolimbic regions is consistent with more effective extinction learning as a result of better vmPFC modulation of the amygdala (supporting online text, figs. S3 and S4).

These experiments identify a behavioral phenotype related to BDNF Val66Met across species providing evidence for translation from mouse to human. The mouse model provides the opportunity to test dose-dependent effects of the BDNF Met allele in both a controlled genetic and environmental background not feasible in humans. These features allow for reliable assignment of behavioral differences to the effects of the Val66Met polymorphism. The human behavioral and imaging findings provide confidence that cross-species translation is biologically valid, by defining the underlying neural circuitry of the behavioral effects of BDNF Val66Met that can be mapped onto known circuits involved in fear learning and extinction. The robustness of our findings across species and paradigms is evidenced by work showing slower extinction coupled with decreased neuronal dendritic complexity in vmPFC in the $BDNF^{Met/Met}$ mice in a conditioned taste aversion task compared with wild-type counterparts (*31*). Furthermore $BDNF^{Met/Met}$ mice exhibit a trend toward blunted expression of c-Fos in the vmPFC as compared with wild-type mice after the fear extinction paradigm (supporting online text and fig. S5).

Impaired extinction learning has been implicated in anxiety disorders, including phobias and posttraumatic stress disorder, whereby the individual has difficulty recognizing an event as safe (*32*). Our neuroimaging findings of diminished ventromedial prefrontal activity and elevated amygdala activity during extinction are reminiscent of those reported in patients with anxiety disorders and depression when presented with an empty threat or aversive stimuli (e.g., fearful faces) (*33*, *34*). Understanding the effect of the BDNF Met allele on specific components of a simple form of learning provides insight into risk for anxiety disorders and has important implications for the efficacy of treatments for these disorders that rely on extinction mechanisms. One such treatment is exposure therapy, whereby an individual is repeatedly exposed to a traumatic event in order to diminish the significance of that event. Our findings suggest that the BDNF Val66Met SNP may play a key role in the efficacy of such treatments and may ultimately guide personalized medicine for related clinical disorders.

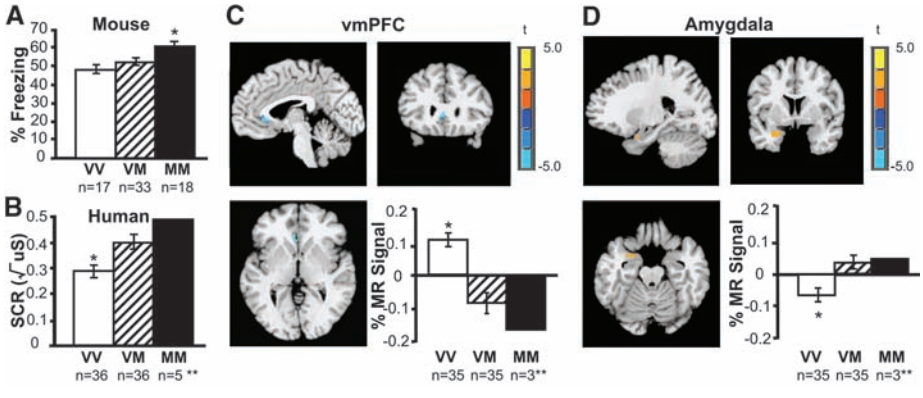

Fig. 3. Neural circuitry of the behavioral effect of BDNF Val66Met during extinction. (**A**) Average percentage of time freezing during extinction by genotype in 68 mice. (**B**) Average skin conductance response (SCR) during extinction by genotype in 72 humans. (**C**) Brain activity as indexed by percent change in magnetic resonance (MR) signal during extinction in the ventromedial prefrontal cortex (vmPFC) by genotype ($x, y, z = -4, 24, 3$), with Met allele carriers having significantly less activity than Val/Val homozygotes (VM < VV is blue), image threshold $P < 0.05$, corrected. (**D**) Genotypic differences in left amygdala activity during extinction ($x, y, z = -25, 2, -20$) in 70 humans, with Met allele carriers having significantly greater activity than Val/Val homozygotes (VM > VV is orange), image threshold $P < 0.05$, corrected. *$P < 0.05$. **MM were included in the analysis with VM, but plotted separately to see the dose response. All results are presented as means ± SEM. VV, Val/Val; VM, Val/Met; MM, Met/Met.

References and Notes

1. Z. Y. Chen *et al.*, *Science* **314**, 140 (2006).
2. M. F. Egan *et al.*, *Cell* **112**, 257 (2003).
3. A. R. Hariri *et al.*, *J. Neurosci.* **23**, 6690 (2003).
4. J. P. Chhatwal, L. Stanek-Rattiner, M. Davis, K. J. Ressler, *Nat. Neurosci.* **9**, 870 (2006).
5. L. M. Rattiner, M. Davis, K. J. Ressler, *Neuroscientist* **11**, 323 (2005).
6. D. S. Charney, H. K. Manji, *Sci. STKE* **2004**, re5 (2004).
7. E. J. Nestler *et al.*, *Neuron* **34**, 13 (2002).
8. M. Gratacòs *et al.*, *Biol. Psychiatry* **61**, 911 (2007).
9. J. M. Gatt *et al.*, *Biol. Psychol.* **79**, 275 (2008).
10. X. Jiang *et al.*, *Neuropsychopharmacology* **30**, 1353 (2005).
11. S. L. Rauch, L. M. Shin, E. A. Phelps, *Biol. Psychiatry* **60**, 376 (2006).
12. S. Lissek *et al.*, *Behav. Res. Ther.* **43**, 1391 (2005).
13. B. O. Rothbaum, M. Davis, *Ann. N. Y. Acad. Sci.* **1008**, 112 (2003).
14. M. R. Delgado, A. Olsson, E. A. Phelps, *Biol. Psychol.* **73**, 39 (2006).
15. F. Sotres-Bayon, C. K. Cain, J. E. LeDoux, *Biol. Psychiatry* **60**, 329 (2006).
16. Materials and methods are available as supporting material on *Science* Online.
17. K. M. Myers, M. Davis, *Neuron* **36**, 567 (2002).
18. G. J. Quirk, E. Likhtik, J. G. Pelletier, D. Paré, *J. Neurosci.* **23**, 8800 (2003).
19. M. R. Milad, G. J. Quirk, *Nature* **420**, 70 (2002).
20. J. E. LeDoux, *Annu. Rev. Neurosci.* **23**, 155 (2000).
21. K. S. LaBar, J. C. Gatenby, J. C. Gore, J. E. LeDoux, E. A. Phelps, *Neuron* **20**, 937 (1998).
22. D. Schiller, I. Levy, Y. Niv, J. E. LeDoux, E. A. Phelps, *J. Neurosci.* **28**, 11517 (2008).
23. M. R. Delgado, K. I. Nearing, J. E. Ledoux, E. A. Phelps, *Neuron* **59**, 829 (2008).
24. R. Kalisch *et al.*, *J. Neurosci.* **26**, 9503 (2006).
25. J. A. Gottfried, R. J. Dolan, *Nat. Neurosci.* **7**, 1144 (2004).
26. E. A. Phelps, M. R. Delgado, K. I. Nearing, J. E. LeDoux, *Neuron* **43**, 897 (2004).
27. K. Nader, J. LeDoux, *Behav. Neurosci.* **113**, 152 (1999).
28. M. Kim, M. Davis, *Behav. Neurosci.* **107**, 580 (1993).
29. K. Lebrón, M. R. Milad, G. J. Quirk, *Learn. Mem.* **11**, 544 (2004).
30. M. R. Milad *et al.*, *Biol. Psychiatry* **62**, 446 (2007).
31. H. Yu *et al.*, *J. Neurosci.* **29**, 4056 (2009).
32. D. S. Charney, *Am. J. Psychiatry* **161**, 195 (2004).
33. I. Liberzon *et al.*, *Biol. Psychiatry* **45**, 817 (1999).
34. S. L. Rauch *et al.*, *Biol. Psychiatry* **47**, 769 (2000).

35. We acknowledge two anonymous reviewers for their thoughtful comments, resources and staff at the

Biomedical Imaging Core Facility of the Citigroup Biomedical Imaging Center at Weill Cornell Medical College, Rafael Oania, a generous gift by the Dr. Mortimer D. Sackler family and support from NIH grants MH079513 (B.J.C., F.S.L.), MH060478 (B.J.C.), NS052819 (F.S.L.), HD055177 (B.J.C., S.S.P.), GM07739 (F.S.), and United Negro College Fund–Merck Graduate Science Research Dissertation Fellowship (F.S.), Burroughs Wellcome Foundation (F.S.L.), and International Mental Health Research Organization (F.S.L.).

Supporting Online Material
www.sciencemag.org/cgi/content/full/science.1181886/DC1
Materials and Methods
SOM Text
Figs. S1 to S5
Tables S1 and S2
References

14 September 2009; accepted 28 December 2009
Published online 14 January 2009;
10.1126/science.1181886
Include this information when citing this paper.

Vibrio cholerae VpsT Regulates Matrix Production and Motility by Directly Sensing Cyclic di-GMP

Petya V. Krasteva,[1] Jiunn C. N. Fong,[2] Nicholas J. Shikuma,[2] Sinem Beyhan,[2] Marcos V. A. S. Navarro,[1] Fitnat H. Yildiz,[2]* Holger Sondermann[1]*

Microorganisms can switch from a planktonic, free-swimming life-style to a sessile, colonial state, called a biofilm, which confers resistance to environmental stress. Conversion between the motile and biofilm life-styles has been attributed to increased levels of the prokaryotic second messenger cyclic di-guanosine monophosphate (c-di-GMP), yet the signaling mechanisms mediating such a global switch are poorly understood. Here we show that the transcriptional regulator VpsT from *Vibrio cholerae* directly senses c-di-GMP to inversely control extracellular matrix production and motility, which identifies VpsT as a master regulator for biofilm formation. Rather than being regulated by phosphorylation, VpsT undergoes a change in oligomerization on c-di-GMP binding.

In *Vibrio cholerae*, biofilm formation is facilitated by colonial morphotype variation (*1*–*4*). Rugose variants produce increased levels of extracellular matrix by means of expression of *Vibrio* polysaccharide (*vps*) genes and genes encoding matrix proteins. *vps* expression is under the control of two positive transcriptional regulators, VpsT and VpsR (*5*, *6*). VpsT is a member of the FixJ, LuxR, and CsgD family of prokaryotic response regulators, typically effectors in two-component signal transduction systems that use phosphoryl transfer from upstream kinases to modulate response-regulator protein activity (*7*–*9*). Although the putative phosphorylation site is conserved in VpsT's receiver domain, other residues crucial for phosphotransfer-dependent signaling are not, and no cognate kinase has been identified to date (fig. S1). Regulation by VpsT and VpsR has been linked to signal transduction by using the bacterial second messenger cyclic di-guanosine monophosphate (c-di-GMP) (*10*, *11*) (fig. S2), yet little is known about the direct targets of the nucleotide. A riboswitch has been identified as a c-di-GMP target that regulates gene expression of a small number of genes, but that is unlikely to account for the global change in transcriptional profile required for biofilm formation (*12*). Neither do PilZ domain–containing proteins, potential c-di-GMP effectors, affect rugosity, because a *V. cholerae* strain lacking all five PilZ domain–containing proteins retains its colony morphology and ability to overproduce *vps* gene products (*13*).

VpsT consists of an N-terminal receiver (REC) domain and a C-terminal helix-turn-helix (HTH) domain, with the latter mediating DNA binding (Fig. 1A) (*14*) (also see supporting online text for details). Unlike other REC domains, the canonical $(\alpha/\beta)_5$-fold in VpsT is extended by an additional helix at its C terminus [helix α6 in (Fig. 1A)]. The HTH domain buttresses an interface formed by helices 3 and 4 of the N-terminal regulatory domain. There are two nonoverlapping dimerization interfaces between noncrystallographic VpsT protomers [chain A-chain B and chain A-chain B^{sym} (symmetrical) in (Fig. 1B)]. The c-di-GMP–independent interface involves interactions mediated by a methionine residue (M^{17}) (*15*) located at the beginning of α1 and a binding pocket that extends into the putative phosphorylation site of the REC domain (fig. S3A). The second interface involves α6 of the REC domain, in contrast to canonical response regulators, such as CheY and PhoB, that utilize a surface formed by α4-β5-α5 for dimerization (*9*). The binding of two intercalated c-di-GMP molecules to the base of α6 stabilizes VpsT dimers using this interface (Fig. 1 and fig. S3B).

The binding motif for c-di-GMP in VpsT consists of a four-residue-long, conserved W[F/L/M][T/S]R sequence (*15*) (fig. S1). The side chains of the tryptophan and arginine form π-stacking interactions with the purine rings of the nucleotide (Fig. 1C). While the hydrophobic residue in the second position plays a structural role where it is buried in the REC domain, the threonine residue at position 3 forms a hydrogen bond with the phosphate moiety of c-di-GMP. A subclass of VpsT and/or CsgD homologs exists with a proline substitution in position 3 (W[F/L/M]PR). Although CsgD is also functionally linked to c-di-GMP signaling in *Escherichia coli* and *Salmonella* (*16*, *17*), its binding pocket appears to be distinct from that of VpsT, as it displays a highly conserved YF[T/S]Q motif that is unlikely to accommodate c-di-GMP (fig. S3B).

The apparent affinity of VpsT for c-di-GMP, determined by isothermal titration calorimetry, is 3.2 μM with 1:1 stoichiometry, consistent with a dimer of c-di-GMP binding to a dimer of VpsT (fig. S4A). Single point mutations in the conserved c-di-GMP–binding motif ($VpsT^{R134A}$, $VpsT^{W131F}$, or $VpsT^{T133V}$) or in the isoleucine in α6 of the c-di-GMP–stabilized REC dimerization interface ($VpsT^{I141E}$) abolished c-di-GMP binding, which indicated that dimeric REC domains are required for binding (fig. S4B). Conversely, mutation of a key residue in the nucleotide-independent interface ($VpsT^{M17D}$) had no effect on c-di-GMP recognition. On the basis of static multiangle light scattering, $VpsT^{M17D}$ exists as a monomeric species in the absence of c-di-GMP, whereas intermediate molecular weights for the wild-type VpsT and the mutants $VpsT^{R134A}$ and $VpsT^{I141E}$ indicated fast exchange between monomers and dimers, presumably through the c-di-GMP–independent interface (fig. S5 and table S2). Addition of c-di-GMP increases the molecular weight of $VpsT^{M17D}$ and wild-type VpsT (figs. S5 and S6), whereas the oligomeric state of $VpsT^{R134A}$ and $VpsT^{I141E}$ is insensitive to the nucleotide.

The role of c-di-GMP recognition and the relevance of the two dimer interfaces in DNA-binding and VpsT-regulated gene expression were assessed by using c-di-GMP binding (R^{134}) and dimerization (I^{141} or M^{17}) mutants (Fig. 2). In electromobility shift assays, we used regulatory sequences upstream of *vpsL*, a gene under positive control of VpsT (Fig. 2A) (*6*). DNA mobility shifts were observed only for the wild-type and $VpsT^{M17D}$ forms, where the effect was protein specific and c-di-GMP dependent. In addition, nucleotide-dependent DNA binding of VpsT was observed to multiple and relatively remote sites in the regulatory region of *vpsL*.

To evaluate the functional importance of VpsT oligomers and c-di-GMP binding in cells, we measured transcription of *vps* genes by using a chromosomal *vpsL*p-*lacZ* transcriptional fusion in the Δ*vpsT* strain harboring wild-type *vpsT*, *vpsT* point mutants ($vpsT^{M17D}$, $vpsT^{R134A}$, or

[1]Department of Molecular Medicine, College of Veterinary Medicine, Cornell University, Ithaca, NY 14853, USA. [2]Department of Microbiology and Environmental Toxicology, University of California, Santa Cruz, CA 95064, USA.

*To whom correspondence should be addressed: yildiz@metx.ucsc.edu (F.H.Y.); hs293@cornell.edu (H.S.)